Published in final edited form as:
Cancer Res. 2010 July 1; 70(13): 5618–5627. doi:10.1158/0008-5472.CAN-09-3740.

Atoh1 inhibits neuronal differentiation and collaborates with Gli1 to generate medulloblastoma-initiating cells

Olivier Ayrault[1], **Haotian Zhao**[1], **Frederique Zindy**[1], **Chunxu Qu**[2], **Charles J. Sherr**[1,3], and **Martine F. Roussel**[1,4]

[1]Department of Genetics and Tumor Cell Biology, 262 Danny Thomas Place, Memphis, Tennessee, 38105

[2]Department of Information Sciences, 262 Danny Thomas Place, Memphis, Tennessee, 38105

[3]Howard Hughes Medical Institute at St. Jude Children's Research Hospital, 262 Danny Thomas Place, Memphis, Tennessee, 38105

Abstract

The morphogen and mitogen Sonic Hedgehog activates a Gli1-dependent transcription program that drives proliferation of granule neuron progenitors (GNPs) within the external germinal layer of the postnatally developing cerebellum. Medulloblastomas with mutations activating the Sonic Hedgehog signaling pathway preferentially arise within the external germinal layer, and the tumor cells closely resemble GNPs. Atoh1/Math1, a basic helix-loop-helix transcription factor essential for GNP histogenesis, does not induce medulloblastomas when expressed in primary mouse GNPs that are explanted from the early postnatal cerebellum and transplanted back into the brains of naïve mice. However, enforced expression of Atoh1 in primary GNPs enhances the oncogenicity of cells overexpressing Gli1 by almost three orders of magnitude. Unlike Gli1, Atoh1 cannot support GNP proliferation in the absence of Sonic Hedgehog signaling and does not govern expression of canonical cell cycle genes. Instead, Atoh1 maintains GNPs in a Sonic Hedgehog-responsive state by regulating genes that trigger neuronal differentiation, including many expressed in response to bone morphogenic protein-4. Therefore, by targeting multiple genes regulating the differentiation state of GNPs, Atoh1 collaborats with the pro-proliferative Gli1-dependent transcriptional program to influence medulloblastoma development.

Keywords

cerebellar neurogenesis; Sonic Hedgehog (Shh); tumor-initiating cells; Patched1 (Ptch1); bone morphogenic protein (BMP)

Introduction

GNPs are specified during embryogenesis and undergo transient proliferation in the external germinal layer (EGL) of the developing postnatal cerebellum, after which they exit the cell cycle, migrate inwardly, and differentiate into mature granule neurons (1). Sonic Hedgehog (Shh), released from Purkinje neurons underlying the EGL, negatively regulates the Patched receptor (Ptch1) expressed on GNPs, thereby relieving its repression of Smoothened (Smo) and triggering a signal transduction pathway that targets Gli transcription factors to induce GNP proliferation. Deregulated pathway activation resulting from *Ptch1* inactivation in GNPs,

Footnotes:[4]To whom correspondence should be addressed. martine.roussel@stjude.org.

or from mutations affecting downstream transducers in the Shh signaling pathway, can induce medulloblastomas (MBs) in mice and humans (2). Mutations constitutively activating the Shh signaling pathway can occur either in multipotent cells within the cerebellar ventricular zone or in lineage-committed GNPs in the EGL. MBs manifesting a Shh gene expression "signature" preferentially arise from, and retain the molecular and phenotypic features of, proliferating GNPs (3–7). Yet despite constitutive activation of the Shh signaling pathway, MB-prone GNPs can still undergo cell cycle exit and further neuronal differentiation, suggesting that additional lineage-specific factors are required to maintain potential tumor-initiating progenitors in an undifferentiated, continuously proliferating state.

The basic helix-loop-helix transcription factor Atoh1 (Math1) is a candidate for playing this role. Deletion of *Atoh1* severely compromises GNP histogenesis during cerebellar development (8) and prevents MB development in vivo (9). Atoh1 expression is restricted to proliferating GNPs within the EGL and is increased in that subset of MBs with Shh pathway mutations (3,10–12), suggesting that it may contribute directly to MB development (13,14). However, the role of Atoh1 in preventing differentiation of GNPs and enhancing medulloblastoma formation is in stark contrast to its role as a tumor suppressor and effector of differentiation in other tissues, including the colon (15,16), the sensory epithelium of the inner ear (17), and the fly retina (18). These opposing outcomes may be governed by the availability of other tissue-specific transcription factors and co-regulators with which Atoh1 interacts.

We previously reported that the bone morphogenic proteins (BMP), BMP2 and BMP4, antagonize MB formation in mice by triggering the proteasomal degradation of Atoh1; however, the ensuing cell cycle exit and neuronal differentiation of BMP2/4-treated MB cells can be overridden by enforced Atoh1 expression (19). Here, we now show that while Gli1 expression enables GNPs to proliferate in the absence of Shh, enforced Atoh1 expression is unable to substitute for Shh signaling. We also now demonstrate that by inhibiting neuronal differentiation, constitutive Atoh1 expression greatly enhances the pro-proliferative effects of Shh/Gli1 signaling in transforming primary GNPs to MBs.

Materials and Methods

Gene transduction and orthotopic GNP transplantation

cDNAs for *Gli1*, *Atoh1*, *Atoh1-ER* (a 3' fusion to an estrogen-responsive element engineered to be induced by 4-hydroxytamoxifen (4-HT)), and *Cre* recombinase were cloned into mouse stem cell virus (MSCV) – internal ribosome entry site (IRES) – green fluorescent protein (GFP) or red fluorescent protein (RFP) vectors. Purified GNPs or MB cells infected during the preplating stage or within 24 hours of plating (4×10^6 cells/well) were quantified for marker expression and injected into cerebral cortices of C57BL/6 or CD-1 *nu/nu* mice [all procedures described in (20)]. Nuclear magnetic resonance imaging (MRI) was performed on anesthetized animals (2–3% isoflurane in O_2) using a 7-Tesla Clinscan scanner (Bruker BioSpin MRI GmbH, Germany) equipped with a 12S gradient (BGA12S) and 4-channel phased-array surface coil. Turbo Spin Echo protocols (T_R 2500–3800 ms; T_E 39–42 ms) produced T2 weighted images (sagittal, coronal and axial) using a matrix of 320 × 320 and field of view of 25 × 25 mm. Images were read using Syngo MR B15 software (Siemens, Erlangen, Germany).

Antibody staining, immunoblotting, proliferation analysis, and fluorescence activated cell sorting (FACS)

Protein detection was performed (12,20) with antibodies to Tuj1 (Covance), $p27^{Kip1}$ (BD), NeuN (Millipore), NeuroD1, $p21^{Cip1}$, Actin (Santa Cruz), Atoh1 (Developmental Studies Hybridoma Bank), GFAP and synaptophysin (DAKO), Ki67, Gli1 (Rockland), p53 (Cell Signaling) and Pax6 (Covance). The percentage of NeuN and $p27^{Kip1}$-stained nuclei within at

least 600 GFP-positive cells was calculated. Where indicated, human recombinant BMP4 (R&D; 100 ng/mL) and 4-HT (Invitrogen; 2μM) were added to cultures. Cultured GNPs were incubated with 10 μM bromodeoxyuridine (BrdU) for 1.5 hours with incorporation quantified by staining with a fluorochrome-conjugated antibody to BrdU (APC-BrdU kit, BD Biosciences) and detected by FACS analysis. Sorting of GNPs marked with GFP and RFP was done as previously described (19) except that infected cells were grown in culture for 2 days before sorting and injection into the cerebella of recipient mice. Confocal imaging of immunofluorescence staining of tumors was performed with a Marinas spinning disk confocal imaging system (Intelligene Imaging Innovations/3i, Denver, CO), consisting of a CSUX confocal head (Yokogowa Electric corporation, Japan), 404nm, 488nm and 561 DPSS lasers (Coherent Inc., Santa Clara, CA) and a Carl Zeiss Axio Observer motorized inverted miscroscope (Carl Zeiss MicroImaging, Thornwood, New York). Images were acquired with a Zeiss Plan-Neofluar 40× 1.3 NA DIC objective on a Evolve EMCDD camera (Photometrics, Tuczon, AZ), using SlideBook 5.0 software (3i). Images are maximum intensity projections of z images taken at 0.5 micron intervals.

Microarrays and Q-RT-PCR

Gene expression profiles generated using GeneChip® Mouse Genome 430 2.0 arrays (Affymetrix, Santa Clara, CA) (3,11,14) were normalized using an Affymetrix Mas5 algorithm, and differentially expressed genes were functionally classified using DAVID Bioinformatics Resource 2008 (21). For determining kinetic responses to 4-HT, we applied k-means clustering using Spotfire (v9.1.1.). Q-RT-PCR primers and probes are described in Supplementary Table S1.

Results

Atoh1 accelerates MB development in *Ptch1*$^{+/-}$:*Cdkn2c*$^{-/-}$ tumor-prone mice

MBs arise spontaneously, but with low penetrance and relatively long latency, in mice lacking one allele of the *Ptch1* gene encoding the Shh receptor (2), but tumorigenesis is accelerated when the *Cdkn2c* gene (encoding the Cdk4/6 inhibitor p18^{Ink4c}) is also inactivated (20). To investigate a role for Atoh1 in MB development, we used retroviral vector-mediated gene transfer to enforce expression of either Atoh1 or Gli1 [a direct pro-proliferative target of the Shh signaling pathway (22)] in primary GNPs purified from the cerebella of postnatal (P) day P5–P7 *Ptch1*$^{+/-}$;*Cdkn2c*$^{-/-}$ (C57BL/6 × 129) mice. Both vectors expressed GFP synthesized in *cis* from an IRES. Triturated GNPs purified on Percoll step-gradients were transduced with the vectors and injected immediately thereafter into the cerebral cortices of immunocompromised CD-1 *nu/nu* recipient animals. FACS analysis of infected GNPs performed at the time of transplantation indicated that 20 ± 3 % of the donor cells expressed GFP, enabling us to estimate that individual recipients received ~ 4 ×10^5 marked cells. Mice observed for subsequent tumor development were sacrificed after initial signs of morbidity, and necropsies were performed to document MB formation.

Mice receiving *Ptch1*$^{+/-}$;*Cdkn2c*$^{-/-}$ GNPs infected with a control vector encoding GFP alone developed GFP-marked tumors after a mean latency of 160 days, whereas enforced Gli1 expression significantly shortened the latency and increased the penetrance of MB development (Fig. 1*A*). Surprisingly, enforced expression of Atoh1 in *Ptch1*$^{+/-}$;*Cdkn2c*$^{-/-}$ GNPs had an even more profound effect on tumorigenesis (Fig. 1*A*). In later studies, transduced donor cells explanted from a backcrossed *Ptch1*$^{+/-}$;*Cdkn2c*$^{-/-}$ pure C57BL/6 strain proved equally tumorigenic when transplanted either into the cerebral cortices or cerebella of healthy syngeneic animals. Histopathological analyses confirmed that all tumors were MBs (Fig. 1*B*, panels a and g; Supplementary Figs. S1*A*) that expressed Pax6, a marker of GNPs (Fig. 1*B*, panels f and l, Supplementary Fig. S2). We confirmed that Gli1 and Atoh1 were expressed in

these tumors (Supplementary Fig. S1*B*). Although MBs induced by Gli1 overexpression retained and expressed the wild type *Ptch1* allele, those induced by Atoh1 exhibited no detectable *Ptch1* expression (Supplementary Fig. S1*C*). This implies that, unlike Gli1, Atoh1 does not increase the threshold of Shh signaling and, like tumors arising spontaneously in $Ptch1^{+/-}$ mice (10,20), requires complete loss of *Ptch1* expression to ensure MB formation.

Atoh1 governs expression of genes regulating neuronal differentiation but not cell proliferation

MBs induced after Gli1 transduction continued to express detectable levels of the neuronal differentiation markers, Tuj1, $p27^{Kip1}$, NeuroD1 and NeuN (Fig. 1*B*, panels b–e Supplementary Fig. S1*B*), whereas those induced by Atoh1 expressed reduced levels of these proteins (Fig 1*B*, panels h–k; Supplementary Fig. S1*A*, S1*B*, S2). To quantify differences in gene expression between MBs induced by overexpression of Gli1 and Atoh1, RNAs extracted from each of three MBs arising from $Ptch1^{+/-}$;$Cdkn2c^{-/-}$ GNPs transduced with retroviral vectors expressing either Gli1 or Atoh1 were subjected to Affymetrix microarray analysis (3 chips per sample). Of the total genes that exhibited significant (> 2-fold) up- or down-regulation in tumors overexpressing either Gli1 or Atoh1, about a quarter responded concordantly, whereas many more were differentially regulated (Supplementary Fig S3*A*). To elucidate categorical differences in gene expression between the two MB subsets, genes undergoing greater than 2-fold up- or down-regulation in Atoh1-induced MBs versus Gli1-induced MBs were assigned to functional groups using Gene Ontology (GO, DAVID database) (21). Scrutiny of all differentially regulated genes revealed that the vast majority of them control processes of cell adhesion, morphogenesis, development, neurogenesis, and neuronal differentiation, but not cell proliferation or apoptosis (Supplementary Table S2). A subgroup of genes encoding proteins well recognized to be involved in neuronal differentiation, migration, and adhesion were perturbed by Atoh1 overexpression, whereas genes canonically regulating GNP cell cycle progression were expressed at equivalent levels in both subsets of MBs (Table 1). More specifically, Tuj1, p27Kip1, NeuroD and Tag1, all markers of neuronal differentiation, were downregulated in MBs expressing Atoh1 compared to those overexpressing Gli1. In contrast, Pax6, MycN and Zic1 that identify GNPs were unchanged (Supplementary Fig S3*B*). Thus, although some genes were regulated similarly, the overall consequences of enforced Gli1 and Atoh1 expression in tumor-prone $Ptch1^{+/-}$;$Cdkn2c^{-/-}$ GNPs were markedly different, with Atoh1 having more profound effects on neuronal differentiation.

Atoh 1 and Gli1 transform GNPs into MB-initiating cells

To determine whether Atoh1 and Gli1 might induce MBs even in the absence of other predisposing mutations, we infected primary GNPs from the P5–P7 cerebella of normal C57BL/6 mice with the vector expressing Gli1/GFP alone or together with an Atoh1 vector coexpressing RFP in lieu of GFP. Wild type GNPs infected with a control vector expressing GFP alone or Atoh1/RFP (~2.2×10^5 marked donor cells) failed to induce tumors in the cortices of syngeneic C57BL/6 recipients within 6 months of transplantation (Fig. 2*A*). In contrast, enforced expression of Gli1/GFP in GNPs resulted in “green” tumors that killed 80% of recipient mice within 200 days post-injection ($t_{1/2}$ = 159 days) (Fig. 2*A*). Remarkably, mice receiving primary GNPs engineered to overexpress both Gli1 and Atoh1 invariably and rapidly succumbed to tumors that uniformly expressed both fluorescent markers ($t_{1/2}$ = 26.5 days) (Figs. 2*A* and 2*C* panel b; Table 2). Because mice can survive even with high tumor burdens, we used magnetic resonance imaging (MRI) to monitor tumor growth. No tumors were detectable 5–11 days after transplantation of 224,000 GNPs overexpressing Gli1 alone (Fig. 2*B*, panels a and c), while 46,000 GNPs co-expressing Gli1 and Atoh1 induced detectable tumor masses as early as 5 days after transplantation (Fig. 2*B*, panels b and d). Tumor growth in these cases was so aggressive that recipient animals had to be sacrificed within 2–3 weeks of transplantation (Table 2).

The rapidity with which tumors coexpressing Atoh1/RFP and Gli1/GFP arose suggested that many if not all infected cells were capable of initiating MBs. We therefore conducted limiting dilution experiments to determine the minimal number of marked GNPs necessary to induce MBs in naïve recipient animals. Because sorting of donor cells prior to their transplantation reduces the efficiency of tumor-induction, marked cells were injected immediately after vector transduction. We retained representative aliquots of these cell populations and retrospectively measured the number of primary GNPs that had been infected with retroviruses encoding Gli1/GFP (GFP+) or Gli1/GFP plus Atoh1/RFP (GFP+/RFP+) by FACS analysis 48 hrs after infection. This allowed us to back calculate the numbers of marked cells injected into the brains of recipient animals. Although over 160,000 Gli1/GFP GNPs were required to induce tumors within 14 weeks, mice receiving as few as ~200 GFP+/RFP+ cells succumbed to tumors as early as one month after transplantation (Table 2). Thus, Atoh1 expression enhanced Gli1's ability to transform GNPs by >800-fold and efficiently converted GNPs into tumor-initiating cells.

MBs arising from GNPs infected with retroviruses expressing Gli1/GFP plus Atoh1/RFP overexpressed Gli1 and Atoh1 (Supplementary Fig. S1*B*) and both GFP and RFP (Fig. 2*C*, panels a and b). They expressed Pax6 confirming that the tumor cells arose from GNPs (Fig. 2C, panel g, Supplementary Fig. S2) and relatively low levels of the neuronal differentiation markers Tuj1, Neuro D1, NeuN and $p27^{Kip1}$(Fig. 2*C*, panels c–f; Supplementary Fig. S1*B*, S2). Spectral karyotyping (SKY) of chromosomes of Gli1/Atoh1-accelerated tumors revealed no gross chromosomal anomalies (Supplementary Fig. S4*A*). Although p53 mutations significantly accelerate MBs induced by deregulated Shh signaling (20, 23), MBs induced by enforced coexpression of Gli1 and Atoh1 retained functional p53, which was rapidly induced, together with its transcriptional target $p21^{Cip1}$, after irradiation of primary tumor cells (Supplementary Fig. S4*B*). Together, these findings underscore the synergy between Atoh1 and the Shh signaling pathway in inducing MBs and further reveal that co-expression of Gli1 and Atoh1 is sufficient to guarantee the conversion of primary GNPs into MB-initiating cells.

Atoh1 does not drive GNP proliferation but maintains their mitogenic response to Shh

After birth, Atoh1 expression in the cerebellum depends on Shh signaling and is detected only in proliferating GNPs within the EGL (8,11). Wild type P7 GNPs infected with retroviruses encoding Gli1/GFP or Atoh1/GFP were cultured with or without Shh. Although enforced expression of Gli1 readily stimulated GNP proliferation in the absence of Shh, GNPs infected with the control GFP vector or with a vector expressing Atoh1/GFP failed to proliferate without Shh stimulation and exited the cell cycle (Fig. 3*A*). However, enforced Atoh1 expression enabled a greater fraction of GNPs to reenter the cell cycle after transient Shh deprivation (Fig. 3*B*) and enhanced their overall mitogenic response when they were stimulated continuously by Shh during a seven day culture period (Supplementary Fig. S5*A*). GNPs cultured in the continued presence of Shh can be induced to undergo further neuronal differentiation by BMP4 treatment (19). However, unlike GNPs transduced by a control GFP-expressing vector, those transduced by Atoh1/GFP resisted the effects of BMP4 in inducing the neuronal differentiation markers, NeuN and $p27^{Kip1}$ (Supplementary Fig. S5*B*). When P7 GNPs explanted from mice homozygous for a "floxed" *Atoh1* allele (9,24) were infected with a retrovirus encoding Cre recombinase and GFP, Atoh1 expression was lost (Fig. 3*C*, top panels), and the infected cells exited the cell cycle more rapidly (Fig. 3*C*, bottom panel) and underwent premature differentiation (Fig. 3*D* shows NeuN, a representative marker) even in the continued presence of Shh. Thus, despite the fact that Atoh1, unlike Gli1 alone, is unable to drive proliferation itself, Atoh1 enhances the ability of Shh-driven GNPs to divide by inhibiting cell cycle exit and neuronal differentiation, and thereby maintains their sensitivity to its mitogenic effects.

Atoh1 overrides the neuronal differentiation program induced by BMP

With the goal of extending the identification of Atoh1-regulated genes involved in neuronal differentiation, we performed a kinetic analysis with a 4-HT-inducible Atoh1-ER fusion protein (25). We first introduced Atoh1-ER into various cultured cell lines and confirmed that 4-HT treatment mobilized the transcription factor to the nucleus (Supplementary Fig. S6*A*), leading to its stabilization in complexes with other E-box binding proteins and to efficient induction of an Atoh1-responsive luciferase reporter gene (Supplementary Figs. S6*B* and S6*C*). We next introduced the validated Atoh1-ER vector into primary P7 GNPs, cultured them for 48 hrs in medium containing Shh alone to establish infection, and then added BMP4 to the medium for an additional 24 hrs. 4-HT was added either together with BMP4 (to induce Atoh1-ER for 24 hrs), or 16 or 20 hrs afterwards (yielding 8 hr and 4 hr 4-HT induction periods, respectively); all induced cultures were harvested simultaneously, and total RNA was extracted for subsequent gene expression profiling. As an additional control, primary GNPs transduced with an Atoh1 mutant (R158G) that neither binds to DNA nor activates transcription (Supplementary Fig. S6*C*) were similarly treated and analyzed.

This protocol was based on previous observations that BMP4 induces proteasomal degradation of the endogenous Atoh1 protein to trigger neuronal differentiation, whereas enforced Atoh1 expression in these cells overrides these phenotypic effects (Supplementary Fig S5*B*) (19). Therefore, we reasoned that, in the absence of the endogenous Atoh1 protein, we might catalogue Atoh1-regulated genes that oppose the action of BMP4 on GNPs, acting to block their further neuronal differentiation and to maintain them in a Shh-responsive state. In keeping with these expectations, the expression of endogenous Atoh1 protein in GNPs cultured in the presence of Shh (Fig. 4*A*, panels a–c) was extinguished by BMP4 (Fig. 4*A*, panels d–f). Uninduced GNPs transduced with Atoh1-ER behaved similarly (Fig. 4*A*, panels g–l), but 4-HT treatment maintained robust expression of the fusion protein even in the face of BMP4 treatment (Fig. 4*A*, panels m–r).

Microarray gene expression profiling identified a total of 66 genes that were up-regulated and 123 genes that were downregulated (fold changes >2) in response to Atoh1-ER induction. Representative “heat maps” of each of the top 50 genes in these categories (Fig. 4*B*) indicated that the up- or downregulation of these genes was not transient but progressed over the course of the 24 hr induction period. Introduction of the Atoh1 mutant defective in DNA binding had minimal effects on the expression of these same genes [designated 4M in Fig. 4*B*], implying that viral infection and 4-HT treatment *per se* did not contribute significantly to their regulation. Quantitative RT-PCR was used to validate the expression of a short list of genes differentially regulated by Atoh1-ER (examples are illustrated in Supplementary Fig. S7). Notably, Gli1 gene expression was unaffected by induction of Atoh1-ER, consistent with the notion that it acts in a parallel pathway (19).

Of the 189 genes that showed greater than two-fold changes in expression, 138 could be functionally classified based on their annotation in Gene Ontology using the DAVID bioinformatics resource database (21). Only two biological processes were significantly affected ($P < 0.01$) by Atoh1-ER induction. By far the major class included 43 genes that were assigned to the Cell Differentiation category ($P = 2.12E-06$; Supplementary Table S3). Moreover, of only fifteen genes listed within the Cell Proliferation category ($P = 3.40E-03$), seven were co-classified as affecting cell differentiation as well (denoted by asterisks in Supplementary Table S3). Many of the genes have been previously implicated in BMP2/4 signaling (see Discussion). Therefore, not only is Atoh1 protein turnover and concomitant neuronal differentiation accelerated in response to BMP2/4 (19), but conversely, Atoh1 acutely counters these effects by rapidly inhibiting the expression of a multitude of BMP target genes.

Discussion

Gene expression profiling of human MBs reveals that they can be subdivided into four distinct subgroups, two of which manifest either SHH or WNT pathway upregulation (26–28). In humans, less than a quarter of MBs manifest grossly aberrant SHH pathway activation, but most mouse models of MB, including those studied here, molecularly recapitulate the human SHH subgroup. Mouse MBs with a Shh signature appear to arise from GNPs in the postnatal cerebellum (3–7). In contrast, several lines of evidence suggest that WNT-driven MBs are generated from more primitive embryonic neuronal progenitors (27). The cells that initiate the other classes of human MBs have not been identified.

Shh drives the proliferation of GNPs during postnatal cerebellar development by inducing pro-proliferative genes that include *Gli1*, *Gli2*, the D-type cyclins *Ccnd1* and *Ccnd2*, and *Mycn* (12,29–31). Similarly, *Atoh1* expression correlates with Shh signaling and is specifically increased in mouse and human MBs that exhibit Shh pathway mutations (3,10,11–16). However, despite the fact that Atoh1 expression is restricted to proliferating GNPs within the EGL and is essential for proper cerebellar histogenesis (8), *Atoh1* is not a direct target of either Shh signaling or N-Myc in GNPs but functions in a parallel pathway (15,29). Notably, enforced expression of either N-Myc (31) or Atoh1 alone (this study) in primary GNPs is unable to induce medulloblastoma, although both genes collaborate with the Shh signaling pathway to accelerate tumor onset. A major difference between them is that enforced N-Myc expression in primary GNPs grown in the presence of Shh is unable to counter the effects of BMP4 (15, 32) while Atoh1 can. Unlike GNPs overexpressing Gli1, those forced to express Atoh1, although able to proliferate in the presence of Shh, were unable to proliferate in its absence. Instead, when Shh was transiently removed from the culture medium, Atoh1 overexpression maintained quiescent GNPs in a prolonged Shh-responsive state, thereby synergizing with re-added Shh to enhance subsequent mitogenesis. Conversely, acute deletion of *Atoh1* in GNPs limited their response to Shh and accelerated neuronal differentiation.

When GNPs explanted from MB tumor-prone *Ptch*$^{+/-}$;*Cdkn2c*$^{-/-}$ mice were transduced with vectors encoding either Gli1 or Atoh1 and transplanted into the brains of naïve animals, MB formation was more significantly accelerated by enforced Atoh1 expression. Consistent with the concept that Gli1 is a key arbiter of Shh signaling and that Atoh1 functions in a parallel pathway, MBs arising from Gli1-transduced donor cells did not inactivate the wild-type *Ptch1* allele, whereas its expression was invariably lost in those MBs whose formation was enhanced by Atoh1. Expression of representative neuronal markers (Tuj1, Neuro D1, p27^{Kip1}, NeuN) was significantly reduced in response to Atoh1. Moreover, a detailed analysis of gene expression differences between MBs induced by overexpression of Gli1 and Atoh1 in this setting indicated that the majority of differentially regulated genes control processes of cell adhesion, morphogenesis, development, neurogenesis, and neuronal differentiation, but not cell proliferation or apoptosis. Notably, the levels of expression of prototypic cell cycle genes, including *Ccnd1*, *Ccnd2*, and *Mycn*, each of which can accelerate MB formation in the *Ptch1*$^{+/-}$;*Cdkn2c*$^{-/-}$ background (12), were not significantly different in MBs that were accelerated by Atoh1 versus Gli1. Together, these findings argue that Atoh1 overexpression inhibits the further differentiation of GNPs, thereby extending and enhancing their response to Shh/Gli1 pathway activation.

Shh-induced proliferation is opposed by a parallel BMP2/4-mediated signaling pathway that accelerates exit of GNPs from the cell division cycle and induces their concomitant differentiation (19,32). BMPs trigger the proteasomal degradation of Atoh1, but enforced expression of Atoh1 overrides these BMP-mediated effects (19). To further investigate the mechanism by which Atoh1 antagonizes the differentiation-inducing effects of BMP2/4, we used a tamoxifen-inducible Atoh1-ER gene to override the effects of BMP4 on GNP gene

expression and again applied microarray gene expression profiling to identify Atoh1-responsive genes. The protocol employed for this experiment minimized expression of the endogenous cellular *Atoh1* gene and allowed a kinetic analysis of genes that responded rapidly to conditional Atoh1 induction. An unsupervised functional classification of Atoh1-ER-responsive genes that exhibited at least two-fold variations in expression identified 189 unique genes, 43 of which regulated cell differentiation and only 15 of which were annotated as ones controlling cell proliferation. Indeed, almost half of the latter were also categorized as governing differentiation processes. Included among these was a group of downregulated genes previously implicated in regulating BMP2/4 signaling, including *Dlx1* and *Dlx2* (33–35), *Hhip* (36), *Runx2* (37–39), *Tbx1* (40), as well as genes such as *Ntn1* and Slit that govern axon guidance (41) and *Cxcr4*, which encodes a G protein-coupled chemokine receptor that regulates GNP migration within the EGL (42). Otx2, the expression of which is essential for proper cerebellar development and has been found to be overexpressed in human medulloblastoma cell lines (43,44) was overexpressed in half of the MBs that arose spontaneously in tumor prone mice exhibiting Shh pathway activation; however, its expression was not significantly changed in Gli1/Atoh1 overexpressing tumors. Moreover, although Flora and collaborators recently reported that Atoh1 can directly induce Gli2 (9), we failed to see an increase in Gli2 transcription after 4HT-mediated Atoh1-ER induction in primary GNPs. Pretreatment of cells with BMP prior to Atoh1 induction and/or variations in the timing of Gli2 induction in the different experimental settings might well account for the apparent discrepancies. We conclude that Atoh1 protein turnover and concomitant neuronal differentiation is not only accelerated in response to BMP2/4 signaling (19), but conversely, that Atoh1 counters these effects by inhibiting the expression of many differentiation-specific genes, BMP targets among them.

Most striking, the enforced co-expression of Atoh1 and Gli1 in primary GNPs explanted from the early postnatal cerebella of healthy C57BL/6 mice guaranteed their conversion into tumor-initiating cells, less than 200 of which induced MBs within two weeks of transplantation into the brains of naïve recipient animals. Remarkably, Gli1 and Atoh1 together appear sufficient to transform primary GNPs into MB-initiating cells. The fact that Atoh1 alone was incapable of inducing MBs in this assay but maximized the oncogenic potential of Gli1 underscores how anti-differentiative and pro-proliferative programs can synergize in initiating cancer.

Supplementary Material

Refer to Web version on PubMed Central for supplementary material.

Acknowledgments

We thank Mary-Elizabeth Hatten, Michael Dyer and Suzanne Baker for constructive criticisms of the manuscript; Jerold Rehg, Dorothy Bush and David Elisson for immunohistochemistry and pathologic review; Richard A. Ashmun and Ann-Marie Hamilton-Easton for flow cytometric analysis; Melissa Johnson and John Killmar for help with orthotopic transplants; Jennifer Peters for confocal imaging of tumors; and Ziwei Zhang and Chris Calabrese for MRI. Robert Johnson, Jennifer Craig, Deborah Yons, Shelly Wilkerson and Sarah Gayso provided excellent technical assistance. We thank Roger Tsien for RFP cDNA; Jane Johnson for the monoclonal antibody to Atoh1; and Huda Zoghbi for supplying “floxed” Atoh1 mice.

Grant Support: This study was supported by NIH grant CA-096832 (MFR) and Cancer Core Grant CA-21765 (MFR/CJS), the Gephardt Endowed Fellowship (OA), American Brain Tumor Association Fellowship (HZ), and the American Lebanese Syrian Associated Charities (ALSAC) of St. Jude Children’s Research Hospital. CJS is an Investigator of the Howard Hughes Medical Institute.

References

1. Sillitoe RV, Joyner AL. Morphology, molecular codes, and circuitry produce the three-dimensional complexity of the cerebellum. Annu Rev Cell Dev Biol 2007;23:549–577. [PubMed: 17506688]

2. Wechsler-Reya R, Scott MP. The developmental biology of brain tumors. Annu Rev Neurosci 2001;24:385–428. [PubMed: 11283316]
3. Lee Y, Miller HL, Jensen P, et al. A molecular fingerprint for medulloblastoma. Cancer Res 2003;63:5428–5437. [PubMed: 14500378]
4. Oliver TG, Read TA, Kessler JD, et al. Loss of patched and disruption of granule cell development in a pre-neoplastic stage of medulloblastoma. Development 2005;132:2425–2439. [PubMed: 15843415]
5. Eberhart CG. Even cancers want commitment: lineage identity and medulloblastoma formation. Cancer Cell 2008;14:105–107. [PubMed: 18691544]
6. Schuller U, Heine VM, Mao J, et al. Acquisition of granule neuron precursor identity is a critical determinant of progenitor cell competence to form Shh-induced medulloblastoma. Cancer Cell 2008;14:123–134. [PubMed: 18691547]
7. Yang ZJ, Ellis T, Markant SL, et al. Medulloblastoma can be initiated by deletion of Patched in lineage-restricted progenitors or stem cells. Cancer Cell 2008;14:135–145. [PubMed: 18691548]
8. Ben-Arie N, Bellen HJ, Armstrong DL, et al. Math1 is essential for genesis of cerebellar granule neurons. Nature 1997;390:169–172. [PubMed: 9367153]
9. Flora A, Klisch TJ, Schuster G, Zoghbi H. Deletion of Atoh1 disrupts Sonic Hedgehog signaling in the developing cerebellum and prevents medulloblastoma. Science 2009;326:1424–1427. [PubMed: 19965762]
10. Berman DM, Karhadkar SS, Hallahan AR, et al. Medulloblastoma growth inhibition by hedgehog pathway blockade. Science 2002;297:1559–1561. [PubMed: 12202832]
11. Akazawa C, Ishibashi M, Shimizu C, Nakanishi S, Kageyama RA. Mammalian helix-loop-helix factor structurally related to the product of the *Drosophila* proneural gene *atonal* is a positive transcriptional regulator expressed in the developing nervous system. J Biol Chem 1995;270:8730–8738. [PubMed: 7721778]
12. Zindy F, Uziel T, Ayrault O, et al. Genetic alterations in mouse medulloblastomas and generation of tumors de novo from primary cerebellar granule neuron precursors. Cancer Res 2007;67:2676–2684. [PubMed: 17363588]
13. Briggs KJ, Corcoran-Schwartz IM, Zhang W, et al. Cooperation between the Hic1 and Ptch1 tumor suppressors in medulloblastoma. Genes Dev 2008;22:770–785. [PubMed: 18347096]
14. Briggs KJ, Eberhart CG, Watkins DN. Just say no to ATOH: how HIC1 methylation might predispose medulloblastoma to lineage addiction. Cancer Res 2008;68:8654–8656. [PubMed: 18974104]
15. Aragaki M, Tsuchiya K, Okamoto R, et al. Proteasomal degradation of Atoh1 by aberrant Wnt signaling maintains the undifferentiated state of colon cancer. Biochem Biophys Res Commun 2008;368:923–929. [PubMed: 18275842]
16. Bossuyt W, Kazanjian A, De Geest N, et al. Atonal homolog 1 is a tumor suppressor gene. PLoS Biol 2009;7:e39. [PubMed: 19243219]
17. Woods C, Montcouquiol M, Kelley MW. Math1 regulates development of the sensory epithelium in the mammalian cochlea. Nature Neurosci 2004;7:1310–1317. [PubMed: 15543141]
18. Bossuyt W, de Geest N, Aerts S, Leenaerts I, Marynen P, Hassan BA. The Atonal proneural transcription factor links differentiation and tumor formation in *Drosophila*. PLoS Biol 2009;e7:e40. [PubMed: 19243220]
19. Zhao H, Ayrault O, Zindy F, Kim JH, Roussel MF. Post-transcriptional down-regulation of Atoh1/Math1 by bone morphogenic proteins suppresses medulloblastoma development. Genes Dev 2008;22:722–727. [PubMed: 18347090]
20. Uziel T, Zindy F, Xie S, et al. The tumor suppressors Ink4c and p53 collaborate independently with Patched to suppress medulloblastoma formation. Genes Dev 2005;19:2656–2667. [PubMed: 16260494]
21. Dennis G Jr, Sherman BT, Hosack DA, et al. DAVID: database for annotation, visualization, and integrated discovery. Genome Biol 2003;4:R60.
22. Kimura H, Stephen D, Joyner A, Curran T. Gli1 is important for medulloblastoma formation in Ptc1 +/− mice. Oncogene 2005;24:4026–4036. [PubMed: 15806168]
23. Wetmore C, Eberhart DE, Curran T. Loss of p53 but not ARF acceleratesmedulloblastoma in mice heterozygous for patched. Cancer Res 2001;61:513–516. [PubMed: 11212243]

24. Shroyer NF, Helmrath MA, Wang VY, Antalffy B, Henning SJ, Zoghbi HY. Intestine-specific ablation of mouse atonal homolog 1 (Math1) reveals a role in cellular homeostasis. Gastroenterology 2007;132:2478–2488. [PubMed: 17570220]
25. Littlewood TD, Hancock DC, Danielian PS, Parker MG, Evan GI. A modified oestrogen receptor ligand-binding domain as an improved switch for the regulation of heterologous recombination. Nucl Acids Res 1995;23:1686–1690. [PubMed: 7784172]
26. Thompson MC, Fuller C, Hogg TL, et al. Genomics identifies subgroups of medulloblastoma that are enriched for specific genetic abnormalities. J Clin Oncol 2006;24:1924–1931. [PubMed: 16567768]
27. Gilbertson RJ, Ellison DW. The origins of medulloblastoma subtypes. Annu Rev Pathol Mech Dis 2008;3:341–365.
28. Northcott PA, Fernandez-L A, Hagan JP, et al. The miR-17/92 polycistron is upregulated in Sonic Hedgehog-driven medulloblastomas and induced by N-Myc in sonic Hedgehog-treated cerebellar neural precursors. Cancer Res 2009;69:3249–3254. [PubMed: 19351822]
29. Lum L, Beachy PA. The hedgehog response network: sensors, switches, and routers. Science 2004;304:1755–1759. [PubMed: 15205520]
30. Katoh Y, Katoh M. Integrative genomic analysis on *GLI1*: positive regulation of GLI1 by Hedgehog-GLI, TGFβ-Smads, and RTK-PI3K-AKT signals, and negative regulation of GLI1 by Notch-CSL-HES/HEY, and GPCR-Gs-PKA signals. Int J Oncol 2009;35:187–192. [PubMed: 19513567]
31. Browd SR, Kenney AM, Gottfried ON, et al. N-Myc can substitute for insulin-like growth factor signaling in a mouse model of Sonic Hedgehog-induced medulloblastoma. Cancer Res 2006;66:2666–2672. [PubMed: 16510586]
32. Rios I, Alvarez-Rodriguez R, Marti E, Pons S. Bmp2 antagonizes sonic hedgehog-mediated proliferation of cerebellar granule neurons through Smad5 signalling. Development 2004;131:3159–3168. [PubMed: 15197161]
33. Locklin RM, Riggs BL, Hicok KC, Horton HF, Byrne MC, Khosla S. Assessment of gene regulation by bone morphogenetic protein 2 in human marrow stromal cells using gene array technology. J Bone Mineral Res 2001;16:2192–2204.
34. Chiba S, Takeshita K, Imai Y, et al. Homeoprotein DLX-1 interacts with Smad4 and blocks a signaling pathway from activin A in hematopoietic cells. Proc Natl Acad Sci USA 2003;100:15577–15582. [PubMed: 14671321]
35. Harris SE, Guo D, Harris MA, Krishnaswamy A, Lichtler A. Transcriptional regulation of BMP-2 activated genes in osteoblasts using gene expression microarray analysis: role of Dlx2 and Dlx5 transcription factors. Front Biosci 2003;8:1249–1265.
36. Katoh Y, Katoh M. Comparative genomics on HHIP family orthologs. Int J Mol Med 2006;17:391–395. [PubMed: 16391842]
37. Wang Q, Wei X, Zhu T, et al. Bone morphogenetic protein 2 activates Smad6 gene transcription through bone-specific transcription factor Runx2. J Biol Chem 2007;282:10742–10748. [PubMed: 17215250]
38. Javed A, Bae JS, Afzal F, et al. Structural coupling of Smad and Runx2 for execution of the BMP2 osteogenic signal. J Biol Chem 2008;283:8412–8422. [PubMed: 18204048]
39. Teplyuk NM, Galindo M, Teplyuk VI, et al. Runx2 regulates G protein-coupled signaling pathways to control growth of osteoblast progenitors. J Biol. Chem 2008;283:27585–27597. [PubMed: 18625716]
40. Fulcoli FG, Huynh T, Scambler PJ, Balsini A. Tbx1 regulates the BMP-Smad1 pathway in a transcription independent manner. PLoS One 2009;4:e6049. [PubMed: 19557177]
41. Killeen MT, Sybingco SS. Netrin, Slit, and Wnt receptors allow axons to choose the axis of migration. Dev Biol 2008;323:143–151. [PubMed: 18801355]
42. Zou YR, Kottmann AH, Kuroda M, Taniuchi I, Littman DR. Function of the chemokine receptor CXCR4 in haematopoiesis and in cerebellar development. Nature 1998;393:595–599. [PubMed: 9634238]
43. de Haas T, Oussoren E, Grajkowska W, et al. OTX1 and OTX2 expression correlates with the clinicopathologic classification of medulloblastomas. J Neuropathol Exp Neurol 2006;65:176–186. [PubMed: 16462208]

44. Adamson DC, Shi Q, Wortham M, et al. OTX2 Is critical for the maintenance and progression of Shh-independent medulloblastomas. Cancer Res 2009;70:181–181. [PubMed: 20028867]

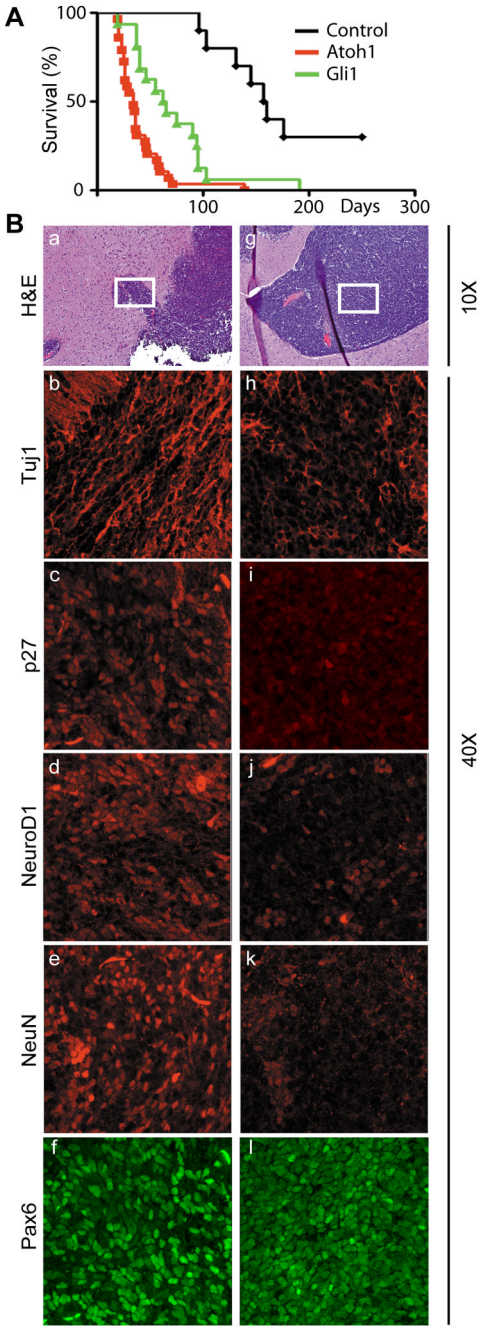

Figure 1.

Atoh1 accelerates MB formation and inhibits neuronal differentiation. (*A*) Survival curves of orthotopically transplanted mice that received GNPs from tumor-prone *Ptch1*$^{+/-}$;*Cdkn2c*$^{-/-}$ animals (black) or those infected with vectors encoding Atoh1/RFP (red) or Gli1/GFP (green). (*B*) MBs accelerated by Gli1 (panels a–f) or Atoh1 (panels g–l) were visualized by H&E staining (panels a and g), by immunofluorescence for the neuronal markers indicated at the left of panels b–f and h–l,. Magnifications are indicated on the right side of the panels.

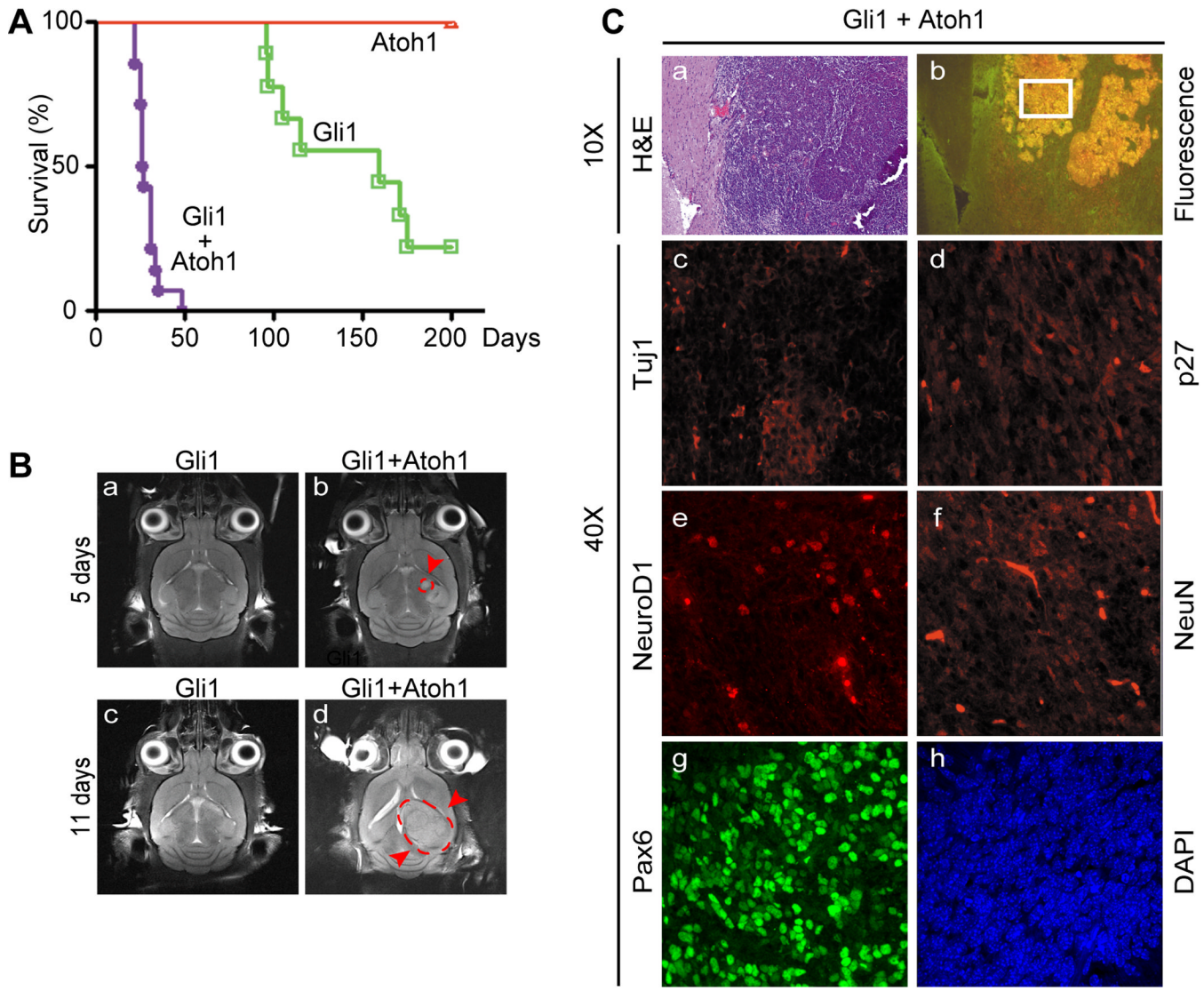

Figure 2.

Atoh1 collaborates with Gli to accelerate MB formation and inhibits neuronal differentiation. (*A*) Survival curves of orthotopically transplanted mice that received primary GNPs explanted from healthy donors. Cells were engineered to express Atoh1/RFP (red), Gli1/GFP (green) or both (purple). (*B*) Magnetic resonance images indicating incipient MBs (red arrows and broken line surrounding the tumor) triggered by GNPs co-expressing Atoh1 and Gli1. Donor cells used in this experiment are indicated by asterisks in Table 1. (*C*) MBs visualized by H&E staining (a) were dually fluorescent (b) and expressed relatively low levels of neuronal markers of differentiation (c–f). Tumor cells were marked by Pax6 (g) and DAPI (h) to visualize nuclei. Magnifications of micrographs are indicated on the left side of the panels.

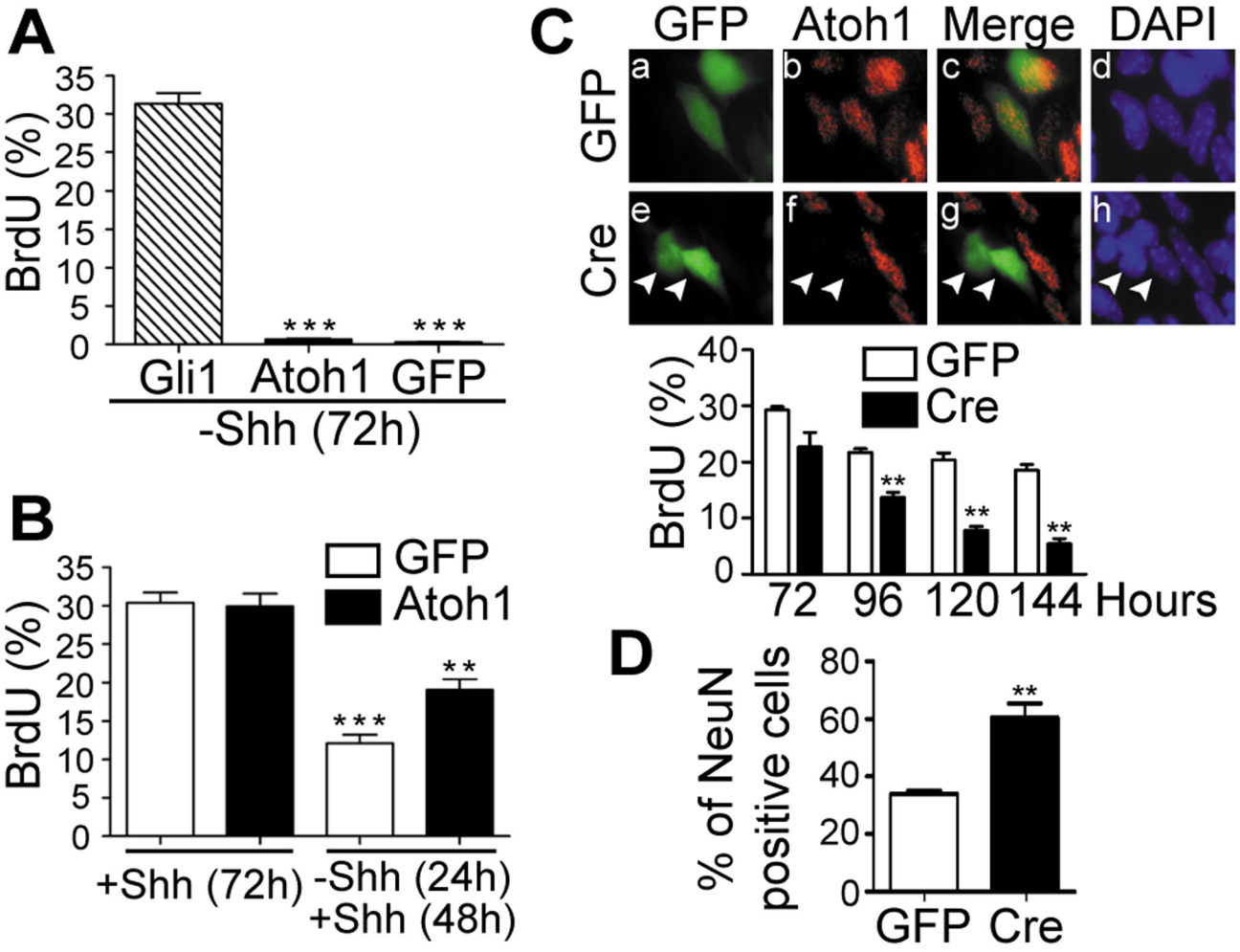

Figure 3.

Atoh1 maintains GNPs in the division cycle but does not directly stimulate proliferation. (*A*) GNPs expressing Gli1/GFP, Atoh1/GFP, or GFP alone were deprived of Shh for 72 hrs, pulsed for 1.5 hrs with BrdU, and the percentage of GFP+ cells that incorporated BrdU was determined by immunofluorescence. (*B*) GNPs expressing GFP alone (white bars) or Atoh1/GFP (black bars) were either maintained in Shh for 72 hrs and labeled with BrdU as above or were deprived of Shh for 24 hrs, restimulated for 48 hrs, and then labeled. (*C, top*) P7 GNPs from "floxed" Atoh1 mice engineered to express GFP alone (panels a–d) or Cre/GFP (panels e–h) (indicated at the left) and cultured in the continued presence of Shh were scored for GFP fluorescence (panels a and e), expression of the endogenous Atoh1 protein by immunofluorescence (panels b and f) (*red*), or stained with DAPI (panels d and h) (*blue*). Panels c and g show merged images of panels a and b and of panels e and f, respectively. Cells expressing Cre noted by arrowheads no longer expressed Atoh1. (*C, bottom*) GNPs infected with GFP control (white bars) or Cre/GFP (black bars) vectors were cultured in presence of Shh for the indicated times (abscissa) and pulsed with BrdU for 1.5 hrs. (*D*) GNPs studied in panel *C* were immunostained for NeuN 120 hrs after infection. For all panels, (***) indicates $P < 0.001$ and (**) $P < 0.01$ (*Student's t-test*).

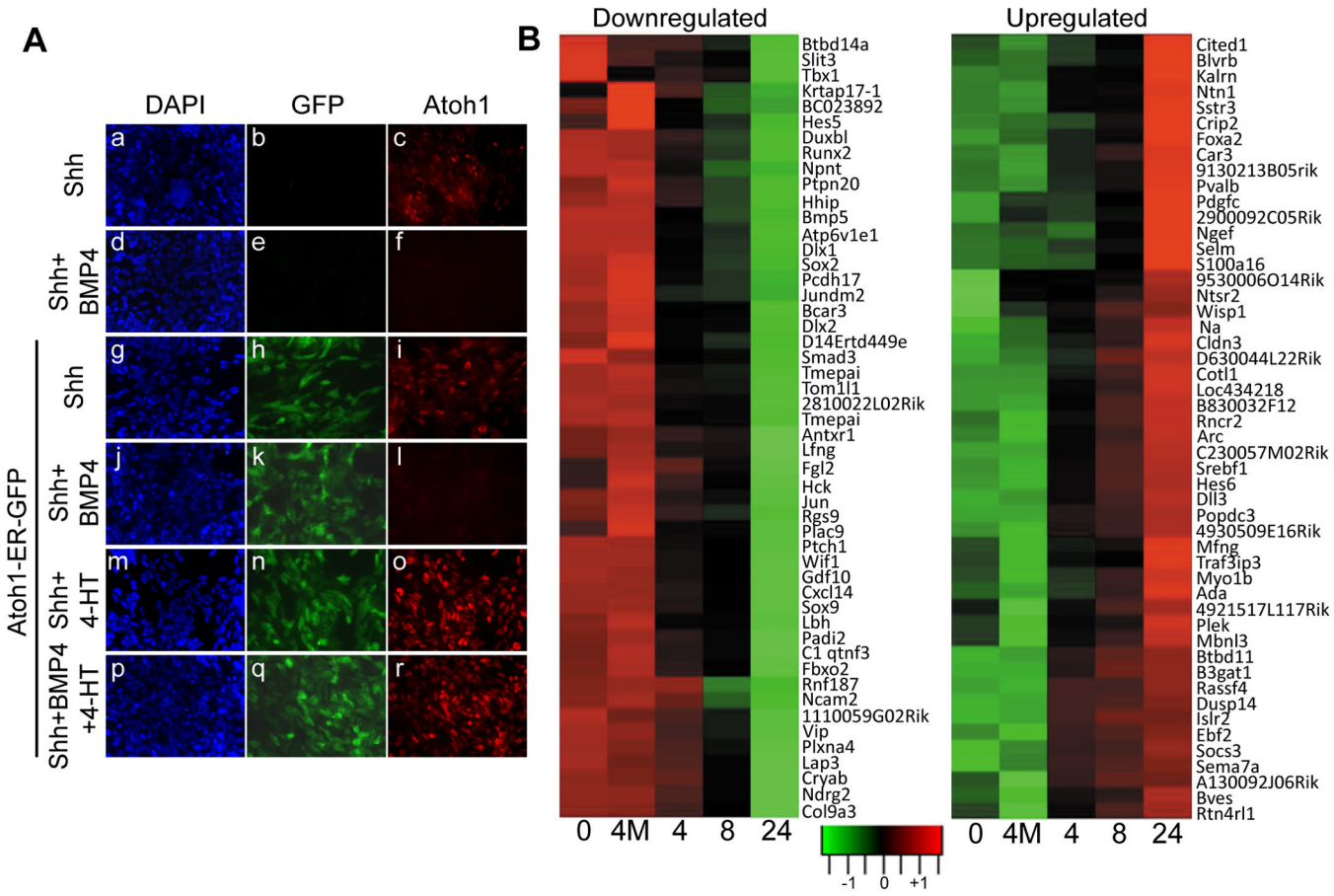

Figure 4.

Downregulation of endogenous Atoh1 protein by BMP4 is overridden by induced Atoh1-ER. (*A*) Untransduced P7 GNPs (panels a–f) or GNPs expressing Atoh1-ER/GFP (panels g–r) were cultured for 24 hrs in Shh with or without BMP4 and/or 4-HT, as indicated at the left of the panels. Cell nuclei were stained with DAPI (*blue*). Vector-encoded GFP was visualized by direct fluorescence (*green*) and Atoh1 by indirect immunofluorescence (*red*). (*B*) GNPs transduced with Atoh1-ER were cultured for an additional 24 hours in Shh and BMP4 to downregulate endogenous Atoh1 expression. 4-HT was added for various times in hours (abscissa) before the conclusion of the experiment to induce Atoh1-ER. As a control, some GNPs were infected with a vector encoding an Atoh1 DNA binding mutant that is transcriptionally inactive (4M). RNAs harvested simultaneously from the cultured cells were used to perform microarray gene expression analysis, illustrated by the “heat maps”. Data obtained for the top 50 downregulated and top 50 up-regulated genes are illustrated. Responsive genes showing greater than two-fold changes in expression from a total of 189 unique genes that were assigned to functional categories ($P < 0.001$) are listed in Supplementary Table 2.

Table 1

Differential Gene Expression in Atoh1-induced versus Gli-induced tumors

Gene Name	Gene Symbol	Fold Change	Gene Function
Differentiation, Migration, Adhesion:			
S100 protein	S100b	− 8.3	Regulation of neuronal synaptic plasticity
Id4	Id4	− 5.6	Inhibitor of DNA binding
Contactin 2	Cntn2, Tag1	− 4.5	Cell adhesion, neuronal migration
Ephrin B2	Efnb2	− 4.3	Cell differentiation, migration
L1cam	L1cam	− 3.8	Adhesion molecule, regulates migration, neurite formation
Nrcam	Nrcam	− 2.5	Surface protein, regulates neurite outgrowth
Cdk5	Cdk5r1, p35	− 2.5	Kinase, regulates migration
Doublecortin	Dcx	− 2.4	Microtubule binding, regulates migration
Plexin B2	Plxnb2	− 2.4	Positive regulation of axon formation
Cadherin 4	Cdh4	+ 4.4	Cell adhesion
Semaphorin 4d	Sem4d	+ 2.7	Cell differentiation and migration
Cell Proliferation:			
Kit Ligand	Kitl	− 4.2	Transient amplifying cell self-renewal
Cyclin D1	Ccnd1	− 0.87	G1 cyclin
Cyclin D2	Ccnd2	−1.7	G1 cyclin
Cyclin A2	Ccna2	+1.1.	G1/S cyclin
Cyclin B1	Ccnb1	+1.1	G2/M cyclin
Cyclin B2	Ccnb2	+1.1	G2/M cyclin
Cell division cycle 25 homolog C	Cdc25c	+1.1	Phosphatase, regulates mitotic entry
Polo-like kinase 1	Plk1	+1.2	Kinase, regulates cell cycle checkpoints
Aurora kinase A	Aurka, Ark1, Stk6	−1.1	Kinase, regulates spindle formation
N-Myc	Mycn	+1.1	Transcription factor
p21, Waf1, Cip1	Cdkn1a	−1.5	CDK inhibitor
p57Kip2	Cdkn1c	−3.0	CDK inhibitor

Table 2

Atoh1 enhances Gli1-mediated transformation of primary GNPs.

Number of marked cells injected	Latency (days) For MB induction
Gli1/GFP	
224,000	96*
160,000	79, 87, 87
120,000	--, --, --
11,200	--, --
Gli1/GFP+Atoh1/RFP	
112,000	14, 14
46,000	13*,19
18,000	14
11,200	16, 18
8,000	14
2,300	19, 40
1,120	21, 21
900	23, 23
224	25, 27, 27
180	33, 59

* indicates tumors shown in Figure 2*B*.